PCCP

Experimental demonstration of necessary conditions for X-ray induced synthesis of cesium superoxide

Journal:	*Physical Chemistry Chemical Physics*
Manuscript ID	CP-ART-10-2022-004767.R1
Article Type:	Paper
Date Submitted by the Author:	02-Dec-2022
Complete List of Authors:	Evlyukhin, Egor; University of Nevada Las Vegas, Department of Physics and Astronomy Cifligu, Petrika; University of Nevada Las Vegas, Department of Physics and Astronomy Pravica, Michael; University of Nevada Las Vegas, Department of Physics and Astronomy Bhowmik, Pradip; University of Nevada Las Vegas, Department of Chemistry and Biochemistry Kim, Eunja; The University of Texas at El Paso, Department of Physics Popov, Dmitry; Argonne National Laboratory X-Ray Sciences Division, High Pressure Collaborative Access Team (HPCAT) Park, Changyong; Argonne National Laboratory X-Ray Sciences Division, High Pressure Collaborative Access Team (HPCAT)

ARTICLE

Experimental demonstration of necessary conditions for X-ray induced synthesis of cesium superoxide

Received 00th January 20xx,
Accepted 00th January 20xx

DOI: 10.1039/x0xx00000x

Egor Evlyukhin,*[a] Petrika Cifligu,[a] Michael Pravica,[a] Pradip K. Bhowmik,[b] Eunja Kim,[c] Dmitry Popov,[d] and Changyong Park[d]

Absorption of sufficiently energetic X-ray photons by a molecular system results in a cascade of ultrafast electronic relaxation processes which leads to a distortion and dissociation of its molecular structure. Here, we demonstrate that only decomposition of powdered cesium oxalate monohydrate induced by monochromatic X-ray irradiation under high pressure leads to the formation of cesium superoxide. Whereas, for an unhydrated form of cesium oxalate subjected to the same extreme conditions, only degradation of the electron density distribution is observed. Moreover, the corresponding model of X-ray induced electronic relaxation cascades with an emphasis on water molecules' critical role is proposed. Our experimental results suggest that the presence of water molecules in initial solid-state systems (i.e. additional electronic relaxation channels) together with applied high pressure (reduced interatomic/intermolecular distance) could potentially be a universal criteria for chemical and structural synthesis of novel compounds via X-ray induced photochemistry.

Introduction

Since the beginning of 20th century, X-ray radiation has been widely utilized for analysis of electronic and structural properties of matter.[1, 2] However, the high proclivity of X-rays to ionize and destabilize atomic/molecular entities via activation of electronic relaxation processes induces damage in matter.[3-7] After the discovery of Auger decay in 1922 and 1925 by Meitner[8] and Auger[9], many more electronic decay processes have been revealed which are driven by electron/electron - Coulomb interaction.[10] These relaxation processes can be distinguished on local (occur within an atomic or molecular entity) and nonlocal (involvement of separated neighboring entities) electronic decays. For instance, during Auger decay, the initially excited atom undergoes autoionization by emitting an electron with a characteristic energy, whereas radiative decay proceeds via emission of characteristic X-rays. Both of these local decays are well-studied and widely used in X-ray and electron-based spectroscopies.[11, 12] On the other hand, only in 1997, Cederbaum and co-workers predicted that in weakly bound matter, for cases where local Auger decay is energetically forbidden due to strong Coulombic repulsion, an excited atom or molecule is able to decay via energy transfer to an atomic or molecular neighbor resulting in its ionization.[13] They termed this process interatomic (or intermolecular) Coulombic decay (ICD). Subsequently, the occurrence of ICD in loosely bound matter was experimentally demonstrated.[14-16] Similar to ICD, a further decay route in loosely bound matter was predicted in 2001 which predominantly occurs in heteronuclear systems; especially in cases where the involved atoms differ strongly in their energetics.[17] This relaxation process was termed electron transfer mediated decay (ETMD). During this decay, an inner-valence or core-shell vacancy in one entity is filled by an electron transfer from a neighboring atom or molecule and the released energy is transferred either to a donor itself or to another neighboring species further ionizing it. Both ICD and ETMD processes depend strongly upon the internuclear/intermolecular distance[10, 17-20] and result in the production of slow electrons which can subsequently ionize the surrounding chemical environment.[21-23]

For the past two decades, electronic relaxation processes have been comprehensively studied from the experimental and theoretical points of view.[10, 18] Particular intention has been devoted toward investigation of the mechanism of ICD and related electron relaxation processes in weakly bound (van der Waals or hydrogen bonding) simple molecular systems in the form of small and large clusters,[19, 24] liquids,[25, 26] as well as in various biological systems.[27, 28] Nevertheless, the ultrafast and probabilistic nature of electronic relaxation processes induced by X-ray photoabsorption,[3] as well as their competitive character (especially for multiphoton induced ionization[29]) significantly complicate the development of experimental and theoretical approaches for their pathways process control. In spite of this, our recent results demonstrate that by a specific selection of initial conditions such as applied high pressure (HP), X-ray source type and X-ray energy, the X-ray induced damage

[a] Department of Physics and Astronomy, University of Nevada Las Vegas, Las Vegas, NV 89154, USA.
[b] Department of Chemistry and Biochemistry, University of Nevada Las Vegas, Las Vegas, NV 89154, USA.
[c] Department of Physics, The University of Texas at El Paso, El Paso, TX 79968, USA
[d] High Pressure Collaborative Access Team (HPCAT), X-Ray Science Division, Argonne National Laboratory, Lemont, IL 60439, USA.

† Footnotes relating to the title and/or authors should appear here.
Electronic Supplementary Information (ESI) available]. See DOI: 10.1039/x0xx00000x

can be controlled and used as a novel approach for materials synthesis.[30, 31]

Previously, we investigated the synthesis of a novel structural form of cesium superoxide (CsO_2) via the synchrotron X-ray induced decomposition reaction of powdered cesium oxalate monohydrate ($Cs_2C_2H_2O_5$) at moderate HPs (≤ 0.5 GPa).[31] It has been observed that under monochromatic X-ray irradiation with energies slightly above or below the K-edge of cesium $Cs_2C_2H_2O_5$ at ambient pressure does not undergo any structural transitions. Whereas at pressures p ≤ 0.5 GPa X-ray irradiation at the same energies induces molecular and structural transformation of the initial material even after several minutes of irradiation. The maximum transformation yield was achieved when samples were irradiated at 36 keV, which is slightly above the K-edge of cesium suggesting that the energy resonance between absorbed X-ray photons and core-shell electrons plays an important role in X-ray induced photochemistry. Although we have demonstrated that HP is a necessary parameter for activation of structural transformations, its role remained unclear. Moreover, the impact of water molecules in the initial compound on the photochemical synthetic pathways has largely been disregarded.

Here, we show that X-ray induced synthesis of CsO_2 proceeds only from the hydrated form of cesium oxalate ($Cs_2C_2H_2O_5$) subjected to HP and no structural and chemical transformations are observed in the case of unhydrated cesium oxalate ($Cs_2C_2O_4$) at the same extreme conditions. Our new experimental results clearly demonstrate that a combination of HP and the presence of water molecules in initial compounds is a critical requirement for synthesis of CsO_2. Furthermore, in this work, we propose a model of a cascade of electronic relaxation processes triggered by X-ray photoionization where we emphasize the critical impact of water molecules. Finally, the HP role is examined in terms of the variations of interatomic distances and X-ray induced transformation rates. We note that cesium oxides are low-work-function semiconductors that play an important role in engineering photoemissive devices[32] and in the activation of catalytic reactions.[33] Therefore, the proposed photochemical synthetic method with its optimized parameters can be suggested for synthesis of novel structural forms of metal oxides which could find wide application in optoelectronics,[34] adaptive oxide electronics,[35-37] and catalytic technologies.[38]

Experimental methods

X-ray-based experiments were performed at the 16 BM-D beamline of the High Pressure Collaborative Access Team (HP-CAT) facilities at the Advanced Photon Source.[39] A tunable Si (111) double crystal in pseudo-channel-cut mode was used as a monochromator to filter ''white'' X-ray radiation and deliver X-rays of fixed but settable energies. Symmetric-style diamond anvil cells (DACs) with 250 μm thick stainless-steel gaskets were employed to confine and pressurize the samples. All samples were loaded into stainless steel gaskets with 100-150 μm diameter holes that were drilled with the laser drilling/micromachining system located at the HPCAT[40] in the preindented 50 μm thickness gasket centers. Powdered cesium oxalate ($Cs_2C_2O_4$) samples (Sigma-Aldrich, purity >99%) were loaded in DACs inside a positive pressure glove box, whereas for investigation of X-ray induced transformations of cesium oxalate monohydrate ($Cs_2C_2H_2O_5$), additional $Cs_2C_2O_4$ samples were loaded in DACs at ambient conditions (outside of a glovebox). We note that $Cs_2C_2O_4$ is extremely hygroscopic; therefore, all $Cs_2C_2O_4$ samples loaded at ambient conditions were immediately transformed into $Cs_2C_2H_2O_5$. This was confirmed by X-ray diffraction. A ruby sphere was loaded with each sample for pressure measurement purposes. No pressure-transmitting medium was used in the experiments. All samples were irradiated for 60 min with monochromatic X-rays at 36 keV energy (λ= 0.3444 Å). The horizontal and vertical full width at half-maximum (FWHM) of the X-ray beam was 5.7 × 4.8 μm. The corresponding photon flux density was 1.08×10^7 photons/(sec×μm^2). Angle-dispersive X-ray diffraction patterns were collected every minute during the X-ray irradiation using a Pilatus®1M detector. The diffraction patterns were integrated in 2-theta using the Dioptas® program,[41] to produce intensity versus 2-theta plots. Interatomic distances were obtained via the CrystalMaker® software.

Results and discussion

Samples of powdered $Cs_2C_2O_4$ were loaded into DACs and irradiated with monochromatic X-rays at 36 keV energy which is slightly above the K-edge of cesium (35.987 keV)[42] at ambient and at high pressures (1.2 GPa and 2.3 GPa). The choice of X-ray energy was defined by our previous study regarding the monochromatic X-ray induced decomposition of $Cs_2C_2H_2O_5$ where the maximum transformation yield was achieved when samples were irradiated at 36 keV.[31] Fig. 1a displays *in situ* XRD patterns of $Cs_2C_2O_4$ at ambient pressure after different X-ray irradiation times. The first XRD pattern, after one minute of irradiation, corresponds to the previously reported monoclinic crystal structure of cesium oxalate with $P2_1/c$ space group and the following lattice parameters: a = 6.62146 Å, b = 11.00379 Å, c = 8.61253 Å, and β = 97.1388° (vertical bars in Fig. 1a).[43] Upon further irradiation, the XRD peak intensities decrease which indicates a distortion of the electron density distribution (XRD patterns 3 - 60 min in Fig. 1a). After 60 min of X-ray irradiation, the overall XRD peak position does not change and no new peaks are detected indicating the absence of formation of a new crystal structure. When $Cs_2C_2O_4$ is subjected to HP, a distortion of the electron density distribution under X-ray irradiation becomes even more pronounced. Figs. 1b and 1c depict *in situ* XRD patterns of $Cs_2C_2O_4$ pressurised to 1.2 GPa and 2.3 GPa after different X-ray irradiation times, respectively. From the initial XRD patterns recorded at ambient and HP after 1 min of X-ray irradiation (Fig. 1 and Fig. S1†) it is evident that pressure by itself does not induce any phase transitions of $Cs_2C_2O_4$ in the 0 – 2.3 GPa pressure range. At HP, all XRD peaks undergo a gradual shift towards higher 2θ indicating a reduction of the unit cell volume. This gradual shift causes the merging of peaks positioned around 5.1° into a single peak and no appearance of new spectral features are detected. The observed HP behaviour

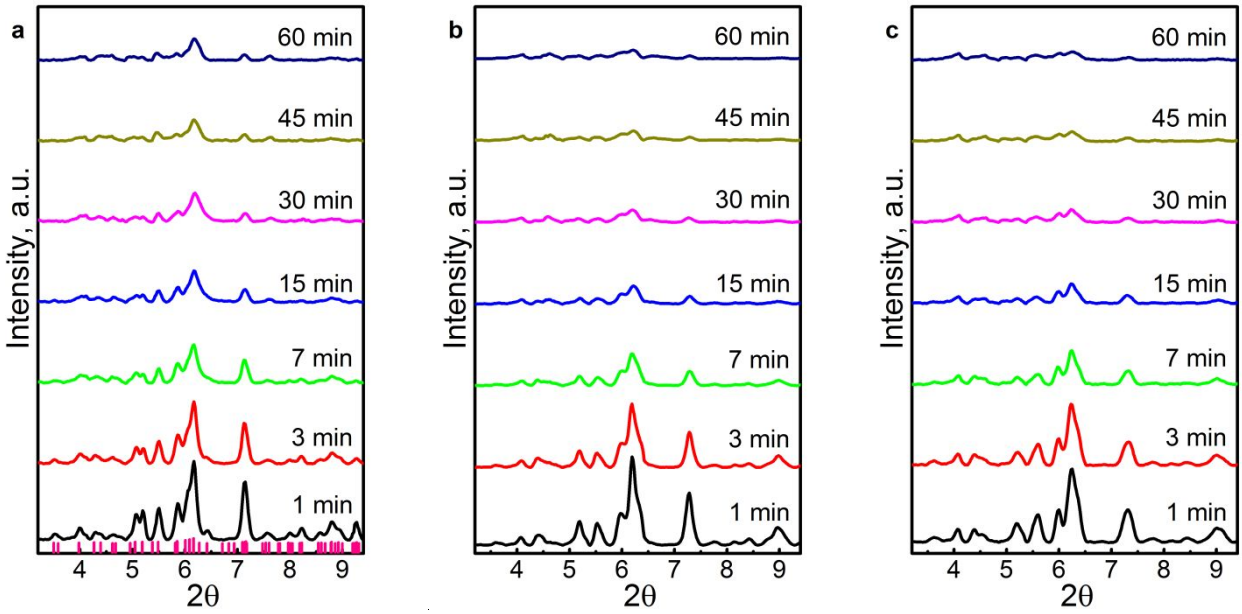

Fig.1. XRD patterns of cesium oxalate after different X-ray irradiation times at 36 keV. (a) $Cs_2C_2O_4$ at ambient pressure; vertical bars indicate peak positions of previously reported monoclinic crystal structure of cesium oxalate.[43] (b) $Cs_2C_2O_4$ at 1.2 GPa and (c) $Cs_2C_2O_4$ at 2.3 GPa.

of $Cs_2C_2O_4$ in the 0 – 2.3 GPa pressure range is consistent with previously reported HP-induced structural evolution of oxalate salts.[30, 44] As can be seen in Figs. 1b and 1c after 60 min of X-ray irradiation, all XRD peaks exhibit much lower intensity in comparison to the initial spectra including the peak at 6.2° which was found to be the most intense peak after 60 min of irradiation at ambient pressure (See Fig. S2†). In both HP cases, consistent with ambient pressure, no formation of new XRD peaks is detected during X-ray irradiation demonstrating that the combination of HP and monochromatic X-rays does not induce synthesis of novel crystalline compound from $Cs_2C_2O_4$. We note that the same X-ray induced behaviour was previously observed for strontium oxalate, barium nitrate and strontium nitrate.[45, 46]

The picture dramatically changes when the hydrated form of cesium oxalate such as $Cs_2C_2H_2O_5$ is used as the initial material. Fig. 2 displays *in situ* XRD patterns of $Cs_2C_2H_2O_5$ at ambient pressure, 0.8 GPa and 2.4 GPa after various X-ray irradiation times at 36 keV. The first XRD pattern obtained after one minute of irradiation at ambient pressure matches with the previously reported monoclinic crystal structure of cesium oxalate monohydrate with $C1_2/c1$ space group and lattice parameters: a = 10.075 Å, b = 6.6473 Å, c = 11.2997 Å, and β = 107.189° (vertical bars in Fig. 2a).[47] Upon further irradiation of $Cs_2C_2H_2O_5$ at ambient pressure, only a decrease of the XRD peaks' intensity is observed indicating a distortion of the electron density distribution (XRD patterns 7 - 60 min in Fig. 2a). The XRD peaks' positions do not change and no new peaks are formed even after 60 min of X-ray irradiation, demonstrating that X-ray exposed $Cs_2C_2H_2O_5$ at ambient pressure does not undergo any structural transformations. This X-ray induced structural behaviour is similar to the previous examples of $Cs_2C_2O_4$ at ambient and HPs indicating that the presence of water molecules in the initial compound does not, in itself, affect its response to X-ray irradiation. However, when $Cs_2C_2H_2O_5$ is subjected to HP, substantial X-ray induced structural transformations occur. Figs 2b and 2c display diffraction patterns of $Cs_2C_2H_2O_5$ at 0.8 GPa and 2.4 GPa after different X-ray irradiation times, respectively. From the initial spectra (1min in Fig. 2 and Fig. S3†), it is apparent that there are no pressure induced structural transformations according to the observed similarity between the patterns. Only a gradual shift towards higher 2θ is noticed indicating the reduction of the unit cell volume with applied HP. Nevertheless, in the first 4 min of X-ray irradiation, at both 0.8 GPa and 2.4 GPa pressures, the diminishing of intensity of all small peaks and merging of the most intense sets of peaks located at near 4.5° and 6.3° are detected (1-4 min patterns in Figs. 2b and 2c). From the 4 min XRD patterns, five of the most intense spectral features located at 4.5°, 6.3°, 7.6°, 8.8° and 9.9° can be distinguished. Upon further irradiation up to 60 min, these XRD peaks undergo a significant growth and at 10 min, a new peak at 11° appears. After 60 min of irradiation, the XRD patterns of $Cs_2C_2H_2O_5$ at 0.8 GPa and 2.4 GPa contain only new peaks and completely different from the initial diffraction patterns as well as from the final XRD pattern of $Cs_2C_2H_2O_5$ at ambient pressure (see Fig. 2 and Fig. S4†). We also note that in the absence of X-ray irradiation no HP induced structural and chemical transformations of $Cs_2C_2H_2O_5$ are observed even after 60 min of applied pressure (see Fig. S5 and Fig. S6). Using *in situ* Raman spectroscopy and DFT calculations we have previously demonstrated that the final product of X-ray irradiated $Cs_2C_2H_2O_5$ at ≤ 0.5 GPa is a mixture of Cs-O derived compounds and its most dominant component cesium superoxide (CsO_2) was found in the *bcc* structural form.[31] The obtained new XRD patterns of $Cs_2C_2H_2O_5$ at 0.8 GPa and 2.4 GPa (60 min in Figs. 2b and 2c) perfectly correspond to this *bcc* structural form of CsO_2 with space group *Pm-3m* and lattice parameter a = 4.5018 Å.

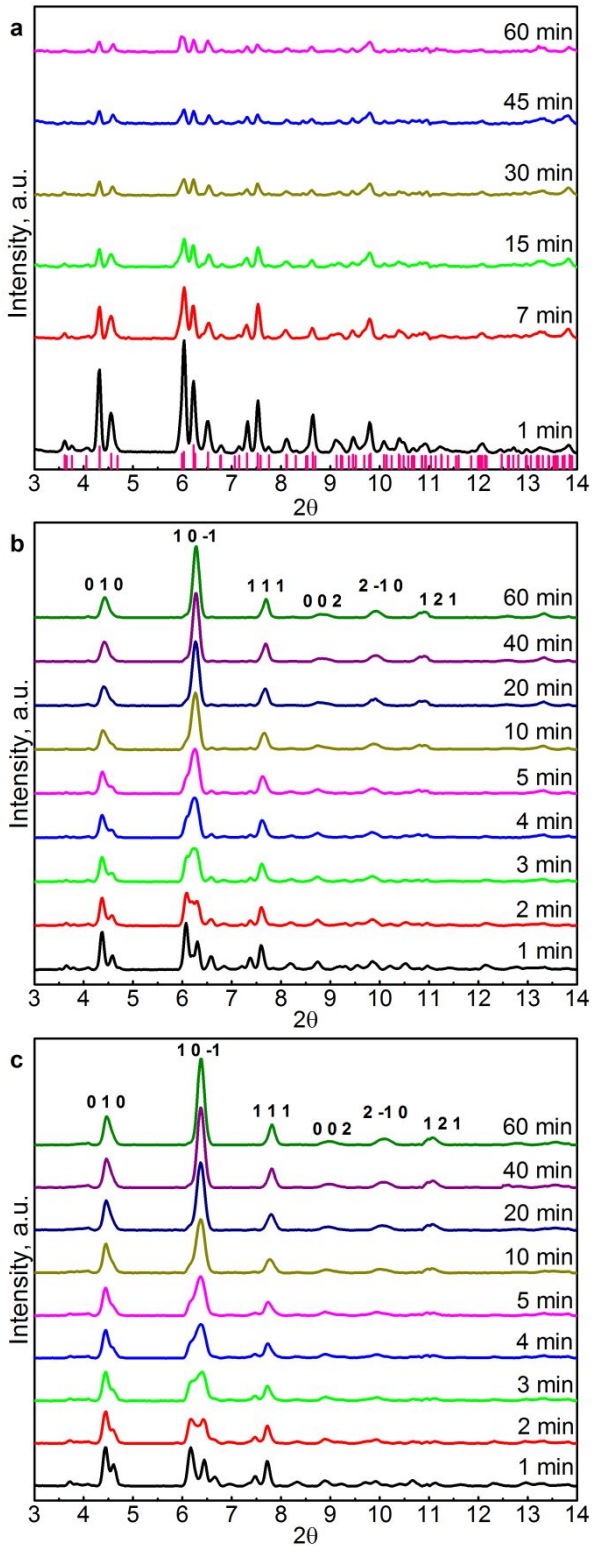

Fig.2. XRD patterns of cesium oxalate monohydrate after different X-ray irradiation times at 36 keV. (a) $Cs_2C_2H_2O_5$ at ambient pressure; vertical bars indicate peak positions of the monoclinic crystal structure of cesium oxalate hydrate[47] (b) $Cs_2C_2H_2O_5$ at 0.8 GPa and (c) $Cs_2C_2H_2O_5$ at 2.4 GPa. Diffraction peaks of the final XRD patterns at 0.8 GPa and 2.4 GPa are labelled with Miller indices of Cs_2O structure with *Pm-3m* space group.[31]

Therefore, our results which include both X-ray induced structural evolutions of $Cs_2C_2O_4$ and $Cs_2C_2H_2O_5$ at ambient and HPs, allow us to conclude that only a combination of HP and the presence of water molecules in initial compound leads the X-ray induced decomposition towards synthesis of a novel structural form of CsO_2.

As mentioned above electronic relaxation processes induced by photoionization are the main factors that cause X-ray induced damage of matter. Therefore, to better understand the critical roles of water molecules as well as HP in X-ray induced photochemistry we have developed a model of the corresponding electronic relaxation cascades triggered by X-ray photoabsorption (see Fig. 3). This model is based on previously reported studies of electronic relaxation processes triggered by X-ray photoionization in weakly bound matter.[3-5, 10, 17, 25] We also note, that earlier, we have proposed another model which describes how electronic relaxation pathways activated in $Cs_2C_2H_2O_5$ depend on the absorbed X-ray energy.[31] We assumed that the energy and electron transfer processes could proceed between the ionically bonded metal cation and oxalate anion. However, electronic relaxation processes such as ICD or ETMD have been theoretically predicted and experimentally observed only in weakly bound matter, where the electronic states of each molecular/atomic entity are localized allowing electron/energy transfer between such entities to take place. On the other hand, when two chemical units are strongly bound (e.g. ionic bond between cation and anion), they cannot be considered as being electronically distinct, thus electron/energy transfer between them is not feasible. Therefore, here we provide a revised model of electronic relaxation processes induced by X-ray photoionization where we also emphasize a critical role of loosely bound water molecules, based upon the experimental results reported in this work. We note that due to the complex nature of ultrafast (femtoseconds) electronic relaxation steps (especially when multiphoton absorption is the main driving phenomenon of X-ray induced damage) it is extremely challenging to cover all possible electronic relaxation pathways. Therefore, in our model we consider the electronic relaxation pathways activated via absorption of one X-ray photon by a metal cation within a single molecule. Nevertheless, we show that even in those cases when the metal cation returns to its initial charge state before photoabsorption, the molecular destabilisation is substantial and the surrounding environment contains a large amount of produced free electrons.

Fig. 3 displays a proposed schematic representation of the electronic decay processes triggered by the absorption of one X-ray photon by a Cs atom, when the photon energy is slightly above the cesium K-edge. X-ray photoabsorption by one Cs^+ cation removes its core shell electron into the surrounding environment and activates a cascade of electronic relaxation steps.[3-5] The pathways and efficiency of electronic relaxation processes depend on the ionization potential of the created excited states.[17] In the case of unhydrated $Cs_2C_2O_4$, there are two possible decay processes (step 1 in Fig. 3): (i) Auger decay[48] (typically dominant in metals) during which an electron with a characteristic energy is emitted by a Cs^{+2} ion which, in turn,

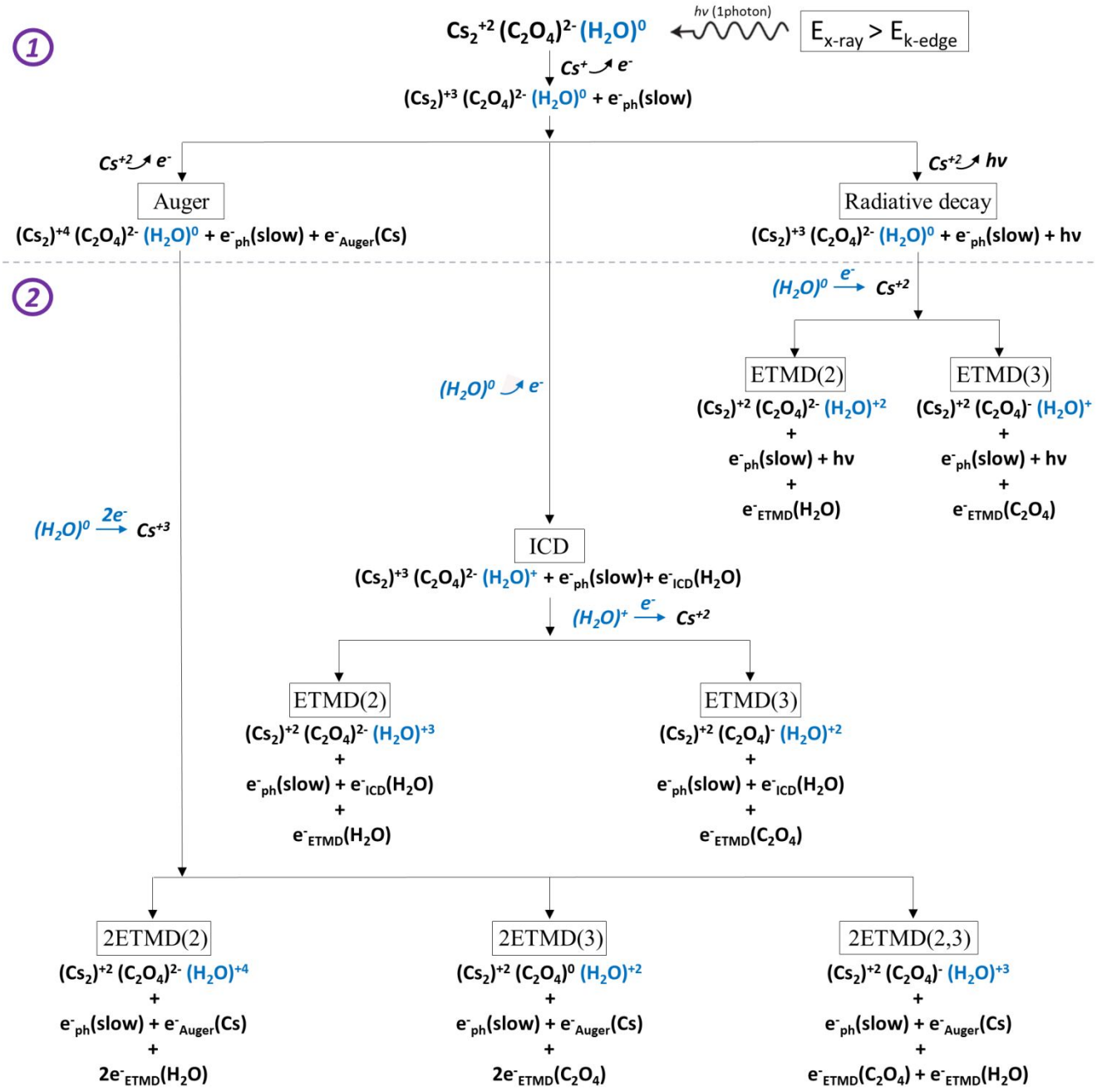

Fig.3. Schematic illustration of the electronic decay processes induced by the absorption of one X-ray photon with energy slightly above the K-edge of Cs by one $Cs_2C_2O_4$ or $Cs_2C_2H_2O_5$ molecule. Labels 1 and 2 represent two major sections in the model: step 1 depict electronic relaxation processes in $Cs_2C_2O_4$, whereas both steps 1 and 2 display electronic relaxation processes in $Cs_2C_2H_2O_5$. After each relaxation step, the change of molecular oxidation states with the type of excited free electrons are presented. ETMD(x) represents the relaxation processes during which an H_2O molecule donates an electron to the Cs^{+2} cation and the excess energy ionizes the donor itself (x=2) or $(C_2O_4)^{2-}$ anion (x=3). 2ETMD(x) represents the relaxation processes during which H_2O molecule donates two electrons to the Cs^{+3} cation.

accumulates a positive charge: Cs^{+3}; and (ii) radiative decay when the excited Cs^{+2} cation decays via the emission of characteristic X-rays (*hv*). At the end of both of these decays the Cs cation is in the excited state (Cs^{+3} or Cs^{+2}) and contains several free electrons in its vicinity, whereas the negatively charged $(C_2O_4)^{2-}$ anion remains its original oxidation state. The created unbound electrons may then secondarily ionize the surrounding environment depending upon their kinetic energy.[21-23] The observed electron density distortion (reduction of the XRD peaks) depicted in Fig. 1 can be explained by this oxidation state destabilisation mechanism within $Cs_2C_2O_4$ molecules induced by X-ray photoabsorption.

When the irradiated system contains weakly bound (hydrogen bonding) water molecules ($Cs_2C_2H_2O_5$), additional electronic relaxation processes become possible (step 2 in Fig.3).[3] Namely, after initial photoionization ($Cs^+ \rightarrow Cs^{2+}$), besides the Auger and radiative decays, an interatomic/intermolecular Coulombic decay (ICD) can be initiated.[10] There are two main contributions of ICD.[23, 49] The direct term during which the Cs^{+2} vacancy is filled by its own outer-shell electron and the excess of energy is transferred to the neighboring H_2O molecule via the classical Coulomb interaction. This interaction is dipole-dipole in type and thus can be viewed as a virtual photon transfer leading to the ionization of the neighbour ($(H_2O)^0 \rightarrow (H_2O)^+$). And, the exchange term in which the Cs^{+2} vacancy is filled by an electron from an H_2O molecule and the excess of energy is used to release a valence electron from the initially ionized Cs atom. After both ICD contributions, the initial oxidation state of $Cs_2C_2H_2O_5$ is identically modified: the Cs cation has a charge state of +2, the C_2O_4 anion remains its original 2- charge state and the water molecule is ionized to +1 oxidation state. Afterwards, ICD as well as radiative decay entail an additional relaxation cascade called electron-transfer-mediated-decay (ETMD).[17] During ETMD, the H_2O molecule donates an electron to Cs^{+2} and the excess of energy ionizes the donor itself (ETMD(2)), or the C_2O_4 anion (ETMD(3)). Moreover, in the presence of water molecules in the initial compound, after Auger decay, several additional ETMD processes are possible: the H_2O molecule donates two electrons to Cs^{+3} and the excess of energy is used to doubly or singly ionize itself or the C_2O_4 anion (2ETMD(2), 2ETMD(3) and 2ETMD(2,3)). As depicted in Fig.3, at the end of all ETMD steps, the cesium atom reverts to its original charge state, the surrounding environment is even more multiply ionized (in comparison to $Cs_2C_2O_4$ case) and contains a larger amount of free electrons suggesting that the presence of water molecules in initial compound plays a critical role in the X-ray induced photochemical reaction pathways. Indeed, our experimental results reported here support this statement as X-ray irradiation led to the formation of crystalline CsO_2 only in the case of $Cs_2C_2H_2O_5$. However, X-ray induced structural transformations were only observed at HP (Fig 2), thus only the combination of HP and the presence of water molecules in the initial compounds is a necessary condition for chemical and structural synthesis via monochromatic X-ray irradiation.

To understand the HP role, it is important to note that the rates of electronic relaxation processes strongly depend on the interatomic/intermolecular distances (R). For instance, the rate of the direct ICD term, which is based on the dipole-dipole interaction, scales with $1/R^6$.[19] On the other hand, in the exchange ICD contribution, orbital overlap is required for an efficient electron transfer, thus, the exchange ICD rate decays exponentially with R.[23] Therefore, the exchange contribution dominates over the direct term at smaller distances. As in the case of ICD and based on the number of involved entities, the decay rate of ETMD also depends on the internuclear/intermolecular distance: ETMD(2) decays exponentially with R, similar to exchange ICD, and ETMD(3) is a superposition of exchange and direct ICDs.[17, 20] Such strong R-dependence of the ICD and ETMD rates suggests that by modulating molecular/atomic separation, for instance via application of HP, it is possible to control the efficiency of the X-ray induced transformation rate.

As discussed earlier, HP by itself does not induce any structural transformations of $Cs_2C_2H_2O_5$ in the pressure range between 0 – 2.4 GPa (Fig.2 and Fig. S4). Therefore, to obtain more insights about the role of HP in X-ray induced photochemistry, every initial XRD pattern of $Cs_2C_2H_2O_5$ (1 min patterns in Fig. 2) were refined and corresponding lattice parameters together with the values of the unit cell volume at 0 GPa, 0.8 GPa and 2.4 GPa are presented in Table 1. Moreover, variations of the interatomic distance between Cs^+ cation and H_2O were obtained via CrystalMaker® software (see Table 1). It is evident that applied pressure reduces the unit cell volume as well as the spatial separation between Cs^+ and H_2O molecules. Therefore, to understand how this effect influences the X-ray induced structural/chemical transformation rate we examined the $Cs_2C_2H_2O_5$ transformation yield (TY) as a function of irradiation time:

$$TY = (Area_t \times 100\%) / Area_{int} \quad (1),$$

where $Area_t$ and $Area_{int}$ are the integrated areas of the XRD patterns obtained after various irradiation times and after 1 min of irradiation, respectively. The X-ray induced *TY* of $Cs_2C_2H_2O_5$ at 0.8 GPa and 2.4 GPa as a function of irradiation time is presented in Fig. 4a. During the first 4 min of X-ray irradiation the TY at both HP points decreases to the same value of ~75 %. However, during the subsequent 56 min of irradiation, the TY at both pressures increases. Moreover, at the end of X-ray irradiation the TY of $Cs_2C_2H_2O_5$ at 0.8 GPa only reaches a value of ~78.1 %, whereas the TY of $Cs_2C_2H_2O_5$ at 2.4 GPa after 60 min of irradiation equals to ~97.3 %. We note that although electronic relaxation processes such as Auger, ICD and ETMD are all in the range of femtoseconds their probabilistic nature strongly depends on the amount of absorbed X-ray photons. Therefore, the observed time scale (minutes to an hour) of the complete X-ray induced chemical and structural transformations of $Cs_2C_2H_2O_5$ at HP is due to a small number of X-ray photons provided in the experiment (10^7 photons/(sec×μm²)). Nevertheless, a drastic TY difference of X-ray induced evolution of $Cs_2C_2H_2O_5$ suggests that HP is not only required for initiation of the structural transformations but also strongly impacts their rates. To obtain the transformation rate (TR) - time dependencies every TY curve was fitted with a polynomial approximation and the first derivatives of these fits were calculated as function of irradiation time. As depicted in Fig. 4b, at 4 min of irradiation, the TR of $Cs_2C_2H_2O_5$ at 2.4 GPa is ~17 times larger than at 0.8 GPa. During the following

Table 1. Values of the lattice parameters, unit cell volume and interatomic distance between Cs^+ cations and H_2O molecule of $Cs_2C_2H_2O_5$ at 0 GPa, 0.8 GPa and 2.4 GPa.

HP, GPa	a (Å)	b (Å)	c (Å)	β (°)	V (Å³)	Cs-H_2O distance (Å)
0	10.22	6.59	11.34	107.68	728.21	3.217
0.8	10.14	6.51	11.26	108.04	707.84	3.190
2.4	10.05	6.39	11.12	108.98	677.03	3.152

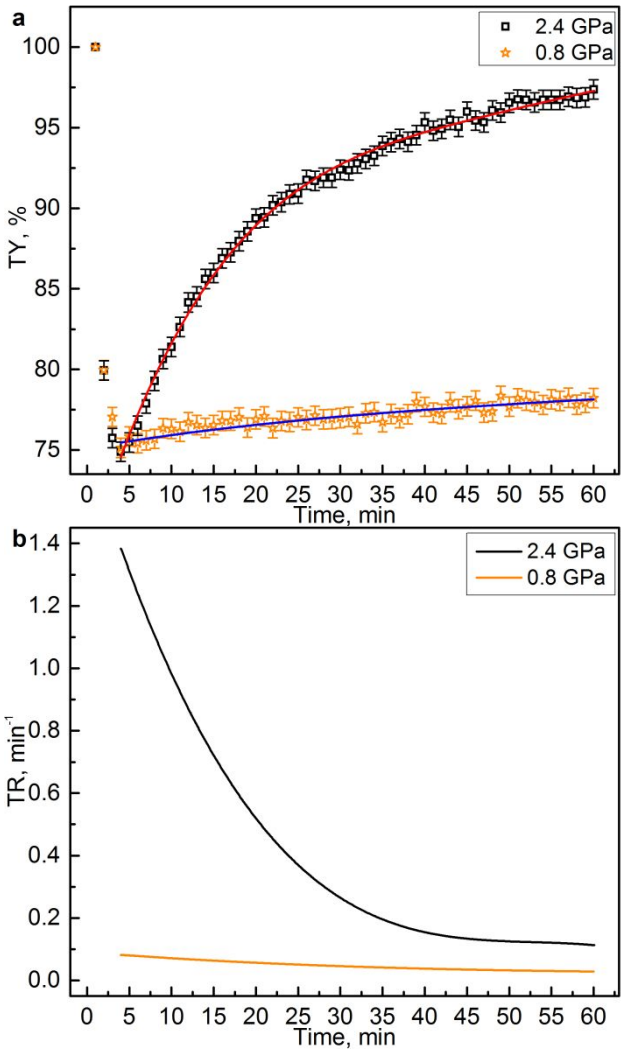

Fig.4. (a) Transformation yield (TY) of $Cs_2C_2H_2O_5$ at 0.8 GPa and 2.4 GPa as function of X-ray irradiation time. The fit curves (red and blue lines) were obtained via polynomial approximation. (b) Transformation rate of $Cs_2C_2H_2O_5$ at 0.8 GPa and 2.4 GPa as function of X-ray irradiation time obtained via differentiation of the fit curves.

irradiation, both rates decay and after 60 min, their ratio is a factor of four. As mentioned earlier, the rates of electronic relaxation processes strongly depend on the interatomic/intermolecular distances. Particularly, at smaller spatial separations electron transfer processes such as exchange ICD and ETMD prevail over the energy transfer decays. Therefore, from our experimental results, we can suggest that with the increase of pressure (reduced Cs-H_2O distance, see Table 1) electron transfer processes between Cs cations and H_2O molecules become more efficient, leading to much more rapid structural transformations of the X-ray irradiated system. It is also important to note that in all ETMD and ICD processes, additional slow electrons are produced. In the presence of a chemical environment, these electrons can be captured by the neutral or ionic entities, activating either nonradiative (due to long-range Coulombic interactions of the electrons)[21] or radiative interatomic/intermolecular Coulombic electron capture processes (ICEC)[22] which further destabilize the molecular system. Therefore, the higher rate of exchange ICD and ETMD induced by HP would result in production of a larger concentration of free electrons causing additional multiple ionizations of the environment and its subsequent dissociation/transformation. We should note that in living tissues, radiation damage occurs within an aqueous environment, therefore, a significant amount of efforts have been devoted for investigation of the water response to ionizing radiation at ambient pressure.[25, 50, 51] Moreover, the formation of an O_2–H_2 alloy from H_2O molecules subjected to X-ray irradiation and HP has also been previously demonstrated.[52] Our results suggest a new potentially useful property of water in X-ray induced photochemistry at HP, where H_2O molecules play a key role as the main electronic relaxation centers.

It is worth mentioning that the X-ray induced decomposition of $Cs_2C_2H_2O_5$ could potentially be investigated by using short intense X-ray pulses provided by X-ray Free-Electron Lasers (XFEL) sources.[53] In this case, an additional information about the dynamics of X-ray induced electronic relaxation processes involved in the chemical mechanisms of CsO_2 formation is expected to be obtained. However, as it was discussed in ref. 54 depending on the pulse duration (e.g. longer than several femtoseconds), the photoelectrons emitted from the ionized atoms could become the dominant destructive forces causing an ejection of the valence electrons from the neighbouring atoms and activating a cascade of the surrounding environment ionisation. For avoiding issues with background of scattered secondary electrons and for investigation of a critical role of electronic relaxation processes in X-ray induced synthesis, for instance ICD, the use of coincidence spectroscopy techniques, such as a cold-target recoil-ion-momentum spectroscopy (COLTRIMS) experiments can be suggested, similar to those conducted on ICD in water dimers/clusters by Jahnke et al. and Mucke et al.[55, 56]

Conclusion

In this work, we experimentally demonstrated that a combination of HP and the presence of water molecules in initial solid-state compound is a necessary requirement for X-ray induced structural and chemical synthesis. Particularly, only the distortion of electron density distribution was observed when unhydrated $Cs_2C_2O_4$ at ambient and HPs was subjected to monochromatic X-ray irradiation and no formation of a novel crystalline compound was detected. On the other hand, only at HP, the X-ray irradiation of $Cs_2C_2H_2O_5$ led to the synthesis of CsO_2 with a bcc structure. In addition, we proposed a model of electronic relaxation processes triggered by X-ray photoabsorption in a single $Cs_2C_2H_2O_5$ molecule with an emphasis on the key role of water molecules. Finally, the critical impact of HP on the X-ray induced transformation rate was examined. Based on the experimental results, it has been suggested that the reduced spatial separation between Cs cations and H_2O molecules increases the rate of electron transfer decay processes, thereby magnifying the rate of X-ray induced synthesis of CsO_2.

Conflicts of interest

There are no conflicts to declare.

Acknowledgements

We gratefully acknowledge support from the Department of Energy, the Basic Energy Sciences (BES) program under Award Number DE-SC0023248. This work was supported in part by State of Nevada UNLV Foundation Catalyst grant (AWD-02-00001154). Portion of this work were performed at HPCAT (Sector 16), APS, Argonne National Laboratory. HPCAT operations are supported by DOE-NNSA's Office of Experimental Sciences. The Advanced Photon Source is a U.S. Department of Energy (DOE) Office of Science User Facility operated for the DOE Office of Science by Argonne National Laboratory under Contract No. DE-AC02-06CH11357. E. E. and P. K. B. sincerely acknowledge the financial support of an industrial sponsored project supported by Koshee Company, Las Vegas, USA. E. K. acknowledges that her research was performed using funding received from the DOE Office of Nuclear Energy's Nuclear Energy University Program under Award Number DE-NE0008788.

References

1. J. Yano and V. K. Yachandra, *Photosynth. Res.*, 2009, **102**, 241-254.
2. A. A. Bunaciu, E. g. Udriştioiu and H. Y. Aboul-Enein, *Crit. Rev. Anal. Chem.*, 2015, **45**, 289-299.
3. V. Stumpf, K. Gokhberg and L. S. Cederbaum, *Nat. Chem.*, 2016, **8**, 237-241.
4. K. Gokhberg, P. Kolorenč, A. I. Kuleff and L. S. Cederbaum, *Nature*, 2014, **505**, 661-663.
5. F. Trinter, M. S. Schöffler, H. K. Kim, F. P. Sturm, K. Cole, N. Neumann, A. Vredenborg, J. Williams, I. Bocharova, R. Guillemin, M. Simon, A. Belkacem, A. L. Landers, T. Weber, H. Schmidt-Böcking, R. Dörner and T. Jahnke, *Nature*, 2014, **505**, 664-666.
6. H. H. Jawad and D. E. Watt, *Int. J. Radiat. Biol. Relat. Stud. Phys. Chem. Med.*, 1986, **50**, 665-674.
7. O. Carugo and K. D. Carugo, *Trends Biochem. Sci*, 2005, **30**, 213-219.
8. L. Meitner, *Eur. Phys. J. A*, 1922, **11**, 35−54.
9. P. Auger, *J. Phys. Radium*, 1925, **6**, 205-208.
10. T. Jahnke, U. Hergenhahn, B. Winter, R. Dörner, U. Frühling, P. V. Demekhin, K. Gokhberg, L. S. Cederbaum, A. Ehresmann, A. Knie and A. Dreuw, *Chem. Rev.*, 2020, **120**, 11295-11369.
11. F. De Groot, *Chem. Rev.*, 2001, **101**, 1779-1808.
12. T. E. Gallon and J. A. D. Matthew, *Rev. Phys. Tech.*, 1972, **3**, 31-64.
13. L. S. Cederbaum, J. Zobeley and F. Tarantelli, *Phys. Rev. Lett.*, 1997, **79**, 4778-4781.
14. T. Jahnke, A. Czasch, M. S. Schöffler, S. Schössler, A. Knapp, M. Käsz, J. Titze, C. Wimmer, K. Kreidi, R. E. Grisenti, A. Staudte, O. Jagutzki, U. Hergenhahn, H. Schmidt-Böcking and R. Dörner, *Phys. Rev. Lett.*, 2004, **93**, 163401.
15. S. Marburger, O. Kugeler, U. Hergenhahn and T. Möller, *Phys. Rev. Lett.*, 2003, **90**, 203401.
16. G. Öhrwall, M. Tchaplyguine, M. Lundwall, R. Feifel, H. Bergersen, T. Rander, A. Lindblad, J. Schulz, S. Peredkov, S. Barth, S. Marburger, U. Hergenhahn, S. Svensson and O. Björneholm, *Phys. Rev. Lett.*, 2004, **93**, 173401.
17. J. Zobeley, R. Santra and L. S. Cederbaum, *J. Chem. Phys.*, 2001, **115**, 5076-5088.
18. T. Jahnke, *J. Phys. B: At. Mol. Opt. Phys.*, 2015, **48**, 082001.
19. V. Averbukh, I. B. Müller and L. S. Cederbaum, *Phys. Rev. Lett.*, 2004, **93**, 263002.
20. C. Buth, R. Santra and L. S. Cederbaum, *J. Chem. Phys.*, 2003, **119**, 10575-10584.
21. K. Gokhberg and L. S. Cederbaum, *J. Phys. Conf. Ser.*, 2012, **388**, 062031.
22. C. Müller, A. B. Voitkiv, J. R. C. López-Urrutia and Z. Harman, *Phys. Rev. Lett.*, 2010, **104**, 233202.
23. T. Jahnke, A. Czasch, M. Schöffler, S. Schössler, M. Käsz, J. Titze, K. Kreidi, R. E. Grisenti, A. Staudte, O. Jagutzki, L. P. H. Schmidt, T. Weber, H. Schmidt-Böcking, K. Ueda and R. Dörner, *Phys. Rev. Lett.*, 2007, **99**, 153401.
24. A. Hans, V. Stumpf, X. Holzapfel, F. Wiegandt, P. Schmidt, C. Ozga, P. Reiß, L. B. Ltaief, C. Küstner-Wetekam, T. Jahnke, A. Ehresmann, P. V. Demekhin, K. Gokhberg and A. Knie, *New J. Phys.*, 2018, **20**, 012001.
25. T. Jahnke, H. Sann, T. Havermeier, K. Kreidi, C. Stuck, M. Meckel, M. Schöffler, N. Neumann, R. Wallauer, S. Voss, A. Czasch, O. Jagutzki, A. Malakzadeh, F. Afaneh, T. Weber, H. Schmidt-Böcking and R. Dörner, *Nat. Phys.*, 2010, **6**, 139-142.
26. O. Marsalek, C. G. Elles, P. A. Pieniazek, E. Pluhařová, J. VandeVondele, S. E. Bradforth and P. Jungwirth, *J. Chem. Phys.*, 2011, **135**, 224510.
27. S. I. Mondal, A. Dey, S. Sen, G. N. Patwari and D. Ghosh, *PCCP*, 2015, **17**, 434-443.
28. P. H. P. Harbach, M. Schneider, S. Faraji and A. Dreuw, *J. Phys. Chem. Lett*, 2013, **4**, 943-949.
29. A. I. Kuleff, K. Gokhberg, S. Kopelke and L. S. Cederbaum, *Phys. Rev. Lett.*, 2010, **105**, 043004.
30. E. Evlyukhin, E. Kim, P. Cifligu, D. Goldberger, S. Schyck, B. Harris, S. Torres, G. R. Rossman and M. Pravica, *J. Mater. Chem. C*, 2018, **6**, 12473-12478.
31. E. Evlyukhin, E. Kim, D. Goldberger, P. Cifligu, S. Schyck, P. F. Weck and M. Pravica, *PCCP*, 2018, **20**, 18949-18956.
32. Y. Sun, Z. Liu, P. Pianetta and D.-I. Lee, *J. Appl. Phys.*, 2007, **102**, 074908.
33. R. J. Davis, *J. Catal.*, 2003, **216**, 396-405.
34. X. Yu, T. J. Marks and A. Facchetti, *Nat. Mat.*, 2016, **15**, 383-396.
35. G. J. Páez Fajardo, S. A. Howard, E. Evlyukhin, M. J. Wahila, W. R. Mondal, M. Zuba, J. E. Boschker, H. Paik, D. G. Schlom, J. T. Sadowski, S. A. Tenney, B. Reinhart, W.-C. Lee and L. F. J. Piper, *Chem. Mater.*, 2021, **33**, 1416-1425.
36. J. L. Andrews, D. A. Santos, M. Meyyappan, R. S. Williams and S. Banerjee, *Trends. Chem.*, 2019, **1**, 711-726.
37. S. A. Howard, E. Evlyukhin, G. Páez Fajardo, H. Paik, D. G. Schlom, L. F. J. Piper, *Adv. Mater. Interfaces*, 2021, **8**, 2001790.
38. J. C. Védrine, *Chinese J. Catal.*, 2019, **40**, 1627-1636.
39. A. Bommannavar, P. Chow, R. Ferry, R. Hrubiak, F. Humble, C. Kenney-Benson, M. Ly, Y. Meng, C. Park, D. Popov, E. Rod, M. Somayazulu, G. Shen, D. Smith, J. Smith, Y. Xiao and N. Velisavljevic, *Phys. Chem. Miner.*, 2022, **49**, 36.
40. R. Hrubiak, S. Sinogeikin, E. Rod and G. Shen, *Rev. Sci. Instrum.*, 2015, **86**, 072202.
41. C. Prescher and V. B. Prakapenka, *High. Press. Res.*, 2015, **35**, 223-230.
42. J. P. Gomilšek, A. Kodre, I. Arčon and M. Hribar, *Phys. Rev. A*, 2003, **68**, 042505.

43. R. E. Dinnebier, S. Vensky, M. Jansen and J. C. Hanson, *Chem. Eur. J*, 2005, **11**, 1119-1129.
44. E. V. Boldyreva, H. Ahsbahs, V. V. Chernyshev, S. N. Ivashevskaya and A. R. Oganov, *Z. Kristallogr. Cryst. Mater.*, 2006, **221**, 186-197.
45. D. Goldberger, E. Evlyukhin, P. Cifligu, Y. Wang and M. Pravica, *J. Phys. Chem. A*, 2017, **121**, 7108-7113.
46. D. Goldberger, C. Park, E. Evlyukhin, P. Cifligu and M. Pravica, *J. Phys. Chem. A*, 2018, **122**, 8722-8728.
47. M. T. Weller, P. F. Henry and M. E. Light, *Acta Cryst.*, 2007, **B63**, 426-432.
48. R. W. Howell, *Int. J. Radiat Biol.*, 2008, **84**, 959-975.
49. R. Santra, J. Zobeley and L. S. Cederbaum, *Phys. Rev. B*, 2001, **64**, 245104.
50. P. Zhang, C. Perry, T. T. Luu, D. Matselyukh and H. J. Wörner, *Phys. Rev. Lett.*, 2022, **128**, 133001.
51. C. Richter, D. Hollas, C.-M. Saak, M. Förstel, T. Miteva, M. Mucke, O. Björneholm, N. Sisourat, P. Slavíček and U. Hergenhahn, *Nat. Commun.*, 2018, **9**, 4988.
52. W. L. Mao, H.-K. Mao, Y. Meng, P. J. Eng, M. Y. Hu, P. Chow, Y. Q. Cai, J. Shu and R. J. Hemley, *Science*, 2006, **314**, 636-638.
53. B. Uwe, J. Kern, R. W. Schoenlein, P. Wernet, V. K. Yachandra, and J. Yano. *Nat. Rev. Phys.*, 2021, **3**, 264–282.
54. H. N. Chapman, *Annu. Rev. Biochem.*, 2019, **88**, 35-58.
55. T. Jahnke, H. Sann, T. Havermeier, K. Kreidi, C. Stuck, M. Meckel, M. Schöffler, N. Neumann, R. Wallauer, S. Voss, A. Czasch, O. Jagutzki, A. Malakzadeh, F. Afaneh, Th. Weber, H. Schmidt-Böcking and R. Dörner, *Nature Phys*., 2010, **6**, 139-142.
56. M. Mucke, M. Braune, S. Barth, M. Förstel, T. Lischke, V. Ulrich, T. Arion, U. Becker, A. Bradshaw and U. Hergenhahn, *Nature Phys*., 2010, **6**, 143-146.